

UDC 621.315.592:548.73

TRANSPORT PROPERTIES OF SINGLE CRYSTALS OF SOLID ELECTROLYTES BASED ON ZrO_2 - Sc_2O_3 CO-DOPED BY SCANDIA, YTTRIA, YTTERBIA AND CERIA

**D.A. Agarkov^{1,2,3}, M.A. Borik³, S.I. Bredikhin^{1,2,3}, I.N. Burmistrov^{1,2,3}, A.S. Chislov^{3,4},
G.M. Eliseeva¹, V.A. Kolotygin¹, A.V. Kulebyakin³, I.E. Kuritsyna^{1,3},
E.E. Lomonova³, F.O. Milovich⁴, V.A. Myzina³, N.Yu. Tabachkova^{3,4}**

¹*Institute of Solid State Physics RAS,*

Academician Osip'yan str. 2, Chernogolovka, Moscow District, 142432 Russia

²*Moscow Institute of Physics and Technology,*

Institutskiy per., 9, Dolgoprudny, Moscow district, 141701 Russia

³*Prokhorov General Physics Institute of the Russian Academy of Sciences,
Vavilov Str. 38, Moscow, 119991 Russia e-mail: lomonova@lst.gpi.ru*

⁴*National University of Science and Technology (MISIS),*

Leninskiy prospekt 4, Moscow, 119049 Russia

Received 28.05.2019

Abstract: Results of structural studies and ionic conductivity of solid solutions $(ZrO_2)_{1-x}(Sc_2O_3)_x$ ($x = 0.08 - 0.10$) doped with 1 mol.% Y_2O_3 , Yb_2O_3 and CeO_2 are presented. Crystals were grown by directional crystallization of melt in cold container. Studies of phase compositions were carried out by means of X-ray diffraction and Raman spectroscopy. Transport properties were studied by impedance spectroscopy in the temperature range of 400–900°C. It was shown that uniform transparent single crystals were obtained only for compositions of $(ZrO_2)_{0.89}(Sc_2O_3)_{0.1}(Y_2O_3)_{0.01}$ and $(ZrO_2)_{0.90}(Sc_2O_3)_{0.09}(Yb_2O_3)_{0.01}$. Stabilization of highly-symmetric phase in crystals co-doped with Yb_2O_3 happens for a lower concentration of Sc_2O_3 in solid solution than for crystals co-doped with Y_2O_3 . Co-doping by ceria did not give an opportunity to obtain the single-phase cubic solid solution. It was also shown, that the conductivity of crystals depends on the amount of Sc_2O_3 in solid solutions. It was detected that conductivity values for tetragonal crystals at 900°C are close and they equal to about 0.1 S/cm by the order of magnitude. Crystals with the composition of $(ZrO_2)_{0.9}(Sc_2O_3)_{0.09}(Yb_2O_3)_{0.01}$ have maximal conductivity in all the temperature range studied. The conductivity value of these crystals at a temperature of 900°C is comparable to the similar value for $(ZrO_2)_{0.9}(Sc_2O_3)_{0.1}$ crystals. However, unlike the $(ZrO_2)_{0.9}(Sc_2O_3)_{0.1}$ crystal containing the rhombohedral phase, the $(ZrO_2)_{0.90}(Sc_2O_3)_{0.09}(Yb_2O_3)_{0.01}$ sample is a single-phase pseudo-cubic.

Keywords: zirconia, ZrO_2 - Sc_2O_3 , crystal growth, ionic conductivity, solid electrolytes, doping, phase analysis

DOI: 10.32737/2221-8688-2019-2-235-245

Introduction

Solid solutions based on ZrO_2 stabilized with Sc_2O_3 are promising materials for use as membranes in solid oxide fuel cells (SOFC). The material shows the highest ionic conductivity among solid solutions of

zirconium dioxide [1-4]. In practice, solid electrolytes are mainly used as gas-tight ceramic membranes manufactured using various ceramic technologies. The functional properties of these ceramic membranes

significantly depend on their microstructure, which, in turn, is controlled by the conditions of the synthesis process. Due to the capabilities of the high-temperature melting method in a cold container [5-8], it is possible to obtain solid solutions based on zirconium dioxide (melting point $\sim 3000^\circ\text{C}$) in the form of single crystals by the method of directional melt crystallization. This approach facilitates the growth of high density monolithic crystalline material with zero porosity and without high-angle grain boundaries.

There are two main problems that limit the practical use of solid solutions based on $\text{ZrO}_2\text{-Sc}_2\text{O}_3$ promising compounds (10-11ScSZ): the existence of a phase transition of the high-temperature cubic phase to the low-temperature rhombohedral in the temperature range of $500\text{-}600^\circ\text{C}$ [1] and the conductivity deterioration over time at working temperatures [9-11].

Experimental procedure

$(\text{ZrO}_2)_{0.99-x}(\text{Sc}_2\text{O}_3)_x(\text{Y}_2\text{O}_3)_{0.01}$, $(\text{ZrO}_2)_{0.99-x}(\text{Sc}_2\text{O}_3)_x(\text{Ce}_2\text{O}_3)_{0.01}$ and $(\text{ZrO}_2)_{0.99-x}(\text{Sc}_2\text{O}_3)_x(\text{Yb}_2\text{O}_3)_{0.01}$ ($x = 0.08\text{-}0.10$) solid solution single crystals were grown by directional crystallization of the melt in a water-cooled copper crucible 130 mm in diameter. ZrO_2 , Sc_2O_3 , Y_2O_3 , Yb_2O_3 and CeO_2 powders of not less than 99.99 % purity grade were used as initial materials. The directional crystallization of the melt was performed by moving the crucible with the melt downward relative to the induction coil at a 10 mm/h rate.

Phase analysis was carried out using Raman scattering spectroscopy on a Renishaw Via Raman spectrometer and home made setup described elsewhere [17-19]. Phase analysis was also performed by means of X-ray diffraction (XRD) on a Bruker D8 diffractometer in $\text{CuK}\alpha$ -radiation with a position sensitive LYNXEYE detector, the DIFFRAC software package and PDF-2 data bank. Phase analysis and measurements of the lattice parameters were carried out on plates cut from crystals perpendicular to the $\langle 100 \rangle$ direction.

One can usually use additional doping of solid solutions of $\text{ZrO}_2\text{-Sc}_2\text{O}_3$, usually by rare-earth elements oxides, to increase the stability of the properties of solid electrolytes. For example, CeO_2 [12-14], Y_2O_3 [10, 15], Yb_2O_3 [14-16], Gd_2O_3 [13-14,16] and Sm_2O_3 [14] were used as co-doping oxides. The results analysis of these studies shows that the properties of the material obtained depend not only on the type and co-doping oxides concentration but also on the method of synthesis of the material.

Purpose of the manuscript

The purpose of this work is to study the effect of co-doping oxides of yttrium, ytterbium and cerium on the phase composition and transport properties of crystals of $(\text{ZrO}_2)_{1-x}(\text{Sc}_2\text{O}_3)_x$ solid solutions ($x = 0.08\text{-}0.10$) obtained by melt crystallization. The co-doping oxides concentration was limited by 1 mol.%.

The ionic conductivity of the crystals was studied in the $623\text{-}1173\text{ K}$ temperature range with 50 K steps using a Solartron SI 1260 frequency analyzer at $1\text{-}5\text{ MHz}$ range and 24 mV AC amplitude signal. The measurements were carried out on crystal plates with the size of $7 \times 7\text{ mm}^2$ and a thickness of 0.5 mm with symmetrically connected platinum electrodes. Platinum electrodes were fired in the air at the temperature of 950°C . The conductivity was estimated in a measurement cell using the four-probe method in a Nabertherm (Nabertherm GmbH, Germany) high-temperature furnace. The impedance frequency spectrum was analyzed in detail using the ZView (ver. 2.8) (Scribner Associates, Inc., USA) software. The crystals conductivity was estimated based on the resultant impedance spectra, and then the specific conductivities of the crystals were calculated. Equivalent circuits described earlier were used for the calculation of the impedance spectra [20].

Results and Discussion

Photos in figure 1 show the appearance of crystals of solid solutions of $(\text{ZrO}_2)_{1-x}(\text{Sc}_2\text{O}_3)_x$ ($x = 0.08-0.10$) co-doped by 1 mol% of Yb_2O_3 (8Sc1YbSZ, 9Sc1YbSZ, 10Sc1YbSZ), 1 mol% Y_2O_3 (8Sc1YSZ, 9Sc1YSZ, 10Sc1YSZ) and 1 mol% of CeO_2

(8Sc1CeSZ, 9Sc1CeSZ, 10Sc1CeSZ). All crystals had a columnar shape typical of this growing method. The size of the crystals in cross section was ~ 20 mm, length of 30-50 mm.



Fig. 1. The appearance of crystals: 8Sc1YbSZ (a), 9Sc1YbSZ (b), 10Sc1YbSZ (c), 8Sc1YSZ (d), 9Sc1YSZ (e), 10Sc1YSZ (f), 8Sc1CeSZ (g), 9Sc1CeSZ (h) and 10Sc1CeSZ (i)

The appearance of the crystals differed depending on the type of co-doping oxide and the concentration of scandium oxide in solid solutions. So ytterbium oxide co-doped crystals (e.g. 8Sc1YbSZ) were uniformly semitransparent without microcracks in the bulk (figure 1a). The transmitted light microstructure images for thin polished plates revealed twins forming during crystal cooling in course of the cubic to tetragonal transition in accordance with the $\text{ZrO}_2\text{-Sc}_2\text{O}_3$ phase diagram. The light-scattering twins made the 8Sc1YbSZ tetragonal crystals opaque and semitransparent. The 9Sc1YbSZ samples were optically homogeneous transparent crystals (figure 1b). The 10Sc1YbSZ samples were semitransparent opalescent crystals without cracks (figure 1c), in the bulk of which a characteristic large block microstructure was clearly distinguishable. Thus, in $(\text{ZrO}_2)_{0.99-x}(\text{Sc}_2\text{O}_3)_x(\text{Yb}_2\text{O}_3)_{0.01}$ crystals, only 9Sc1YbSZ

samples were transparent homogeneous single crystals.

When doping with yttrium oxide, 8Sc1YSZ crystals were almost completely non-uniform and semi-transparent, and only in the upper part of the crystal, corresponding to the end of crystallization, where some small transparent areas were present. In samples 9Sc1YSZ we observed alternation of transparent and muddy areas along with the height of the crystal. Samples 10Sc1YSZ were completely homogeneous transparent single crystals. Completely transparent single crystals with no visible defects were obtained with a higher concentration of scandium oxide in the solid solution of 10 mol%. When doping by 1 mol% of Y_2O_3 in contrast to crystals doped by 1 mol% of Yb_2O_3 .

For doping with cerium oxide in the studied range of compositions it was not possible to obtain optically homogeneous, transparent crystals $(\text{ZrO}_2)_{0.99-x}$

$x(\text{Sc}_2\text{O}_3)_x(\text{CeO}_2)_{0.01}$ in contrast to crystals doped with yttrium and yttrium oxides. The color of the crystals, doped with cerium oxide, was heterogeneous, changing from orange to dark red. The non-uniformity of the color is associated both with a change in the valence state of the cerium ion in the process of cooling the crystal after growth and with fluctuations in the concentration of the admixture of cerium oxide in the crystallization process. In the first case, the heterogeneity manifests itself in the form of a decrease in the color intensity until the appearance of colorless areas on the crystal surfaces, which is most characteristic for crystals grown closer to the periphery of the crystallized melt ingot. Such a color change indicates a decrease in the concentration of the trivalent cerium cation, which has absorption bands in the visible region and gives the crystals an orange color [21]. In the process of cooling the ingot, the $\text{Ce}^{3+} \rightarrow \text{Ce}^{4+}$ transition occurs as oxygen diffuses from the ingot periphery. Another type of color unevenness is associated with fluctuations in the

concentration of cerium oxide in the process of crystallization, manifesting itself in a crystal as stripes with a color of different intensity. This is associated with the displacement of a cerium impurity in the process of crystallization, which has an effective distribution coefficient of less than 1 [21]. Suppression of impurities usually occurs along with the ingot height and the color intensity gradually increases by the end of crystallization. A local increase in the concentration of cerium oxide in the form of individual stripes with an increased color intensity is associated with a disturbance of normal crystallization due to concentration supercooling at the crystallization front, which leads to rapid crystallization of the area enriched by the suppressed impurity.

Thus, at comparable concentrations of scandium oxide and co-doping oxide in solid solutions, the appearance of crystals strongly depends on the type of co-doping oxide. Among the grown crystals, transparent and homogeneous single crystals were obtained only for compositions 9Sc1YbSZ and 10Sc1YSZ.

Table 1. The phase composition and lattice parameters of grown crystals

Sample	Phase composition*	Spacegroup	Lattice parameters		
			a, nm	c, nm	$c/\sqrt{2} a$
8ScSZ	t	$P4_2/nmc$	0.3596(1)	0.5123(1)	1.007
8Sc1YbSZ	t	$P4_2/nmc$	0.3598(1)	0.5113(1)	1.005
8Sc1YSZ	t	$P4_2/nmc$	0.3600(1)	0.5119(1)	1.006
	c	$Fm\bar{3}m$	0.5103(1)		
8Sc1CeSZ	t	$P4_2/nmc$	0.3599(1)	0.5114(1)	1.005
9ScSZ	t	$P4_2/nmc$	0.3595(1)	0.5122(1)	1.007
9Sc1YbSZ	c	$Fm\bar{3}m$	0.5094(1)		
9Sc1YSZ	t	$P4_2/nmc$	0.3600(1)	0.5117(1)	1.005
	c	$Fm\bar{3}m$	0.5095(1)		
9Sc1CeSZ	t	$P4_2/nmc$	0.3597(1)	0.5110(1)	1.005
	c	$Fm\bar{3}m$	0.5092(1)		
10ScSZ	c	$Fm\bar{3}m$	0.5091(1)	0.9010(2)	
	r	$R\bar{3}m$	0.3562(1)		
10Sc1YbSZ	c	$Fm\bar{3}m$	0.5095(1)	0.9003(2)	
	r	$R\bar{3}m$	0.3563(1)		
10Sc1YSZ	c	$Fm\bar{3}m$	0.5096(1)		
10Sc1CeSZ	c	$Fm\bar{3}m$	0.5093(1)	0.9007(2)	
	r	$R\bar{3}m$	0.3560(1)		

**t* – tetragonal modification ZrO_2

c – cubic modification ZrO_2

r – rhombohedral modification ZrO_2

Table 1 shows the phase composition and lattice parameters of the grown crystals according to X-ray diffraction data. For comparison, the data for $(ZrO_2)_{1-x}(Sc_2O_3)_x$ crystals ($x = 0.08-0.10$) are also given.

According to the data obtained by X-ray diffraction, the co-doping of an 8ScSZ crystal with ytterbium and cerium oxides does not change the phase composition. In the 8Sc1YbSZ and 8Sc1CeSZ crystals, there is only a tetragonal ZrO_2 modification, as well as in the 8ScSZ crystal, but there is a change in the parameters of the crystal structure expressed in an increase in the lattice parameter “a” and a decrease in the parameter “c”. The degree of tetragonality in 8Sc1YbSZ and 8Sc1CeSZ crystals is less than in 8ScSZ crystals. Crystals of 8Sc1YSZ, co-doped with yttrium oxide, were biphasic, and the tetragonal and cubic phases were present in them. The cubic phase in 8Sc1YSZ samples was observed only in separate transparent parts of the crystal, corresponding to the end of the melt crystallization. In the main volume of the 8Sc1YSZ crystal, there was a tetragonal phase of zirconium dioxide with a lower degree of tetragonality than the crystals of 8ScSZ. It should be noted that only doping of 8ScSZ with yttrium oxide leads to the appearance of a cubic phase in these crystals. In this case, the lattice parameters of the tetragonal phase of 8ScSZ crystals when doped with yttrium oxide vary less significantly in comparison to the parameters of the tetragonal phase of 8Sc1YbSZ and 8Sc1CeSZ crystals.

The introduction of 1 mol% of Yb_2O_3 into the tetragonal crystal 9ScSZ leads to the stabilization of the cubic phase in the entire crystal volume. According to X-ray diffraction data, 9Sc1YbSZ crystal is a single-phase single crystal with a cubic fluorite structure. The 9Sc1YSZ and 9Sc1CeSZ crystals are biphasic; they are a mixture of regions with a cubic and tetragonal structure. Thus, co-doping of solid solutions of 9ScSZ by 1 mol% of Y_2O_3 or CeO_2 leads to the formation of only separate regions of the cubic phase in the bulk of the crystals.

The phase composition of 10ScSZ, 10Sc1YbSZ and 10Sc1CeSZ crystals is a mixture of regions with cubic and rhombohedral phases. Co-doping of 10ScSZ crystals with ytterbium and cerium oxides did not lead to a change in the phase composition and stabilization of the cubic phase. Only the introduction of yttrium oxide into the composition of the 10ScSZ solid solution gave an opportunity to obtain single-phase cubic single crystals.

Thus, the additional doping of solid solutions $(ZrO_2)_{1-x}(Sc_2O_3)_x$, where ($x = 0.08 - 0.10$) by 1 mol% of ytterbium, yttrium or cerium oxides led to stabilization of the cubic phase in the entire crystal's volume only for 9S1YbSZ and 10S1SZ. In the studied range of compositions, co-doping with cerium oxide did not give the opportunity to obtain a single-phase cubic solid solution. It should be noted that the stabilization of the cubic phase in crystals, co-doped with Yb_2O_3 , occurs at a lower concentration of Sc_2O_3 in the solid solution, than in crystals, co-doped with Y_2O_3 . This may be due to the dependence of the mechanism for stabilizing the high-temperature phase on the type of stabilizing impurity. In $ZrO_2-R_2O_3$ binary systems, a decrease in the ionic radius reduces the transition temperature from the high-temperature cubic phase to the low-temperature tetragonal phase and expands the region of existence of the cubic phase [22], which leads to the preservation of the high-temperature cubic phase at room temperature with a lower concentration of stabilizing oxide. It is possible that this pattern is also valid for the studied triple systems, the data on which are currently very limited.

The phase composition of the grown crystals was also studied by the method of Raman scattering of light. The data on the phase composition obtained by the Raman spectroscopy method are in good agreement with the data obtained by the X-ray diffraction method. Raman spectra of the investigated crystals are presented in figure 2.

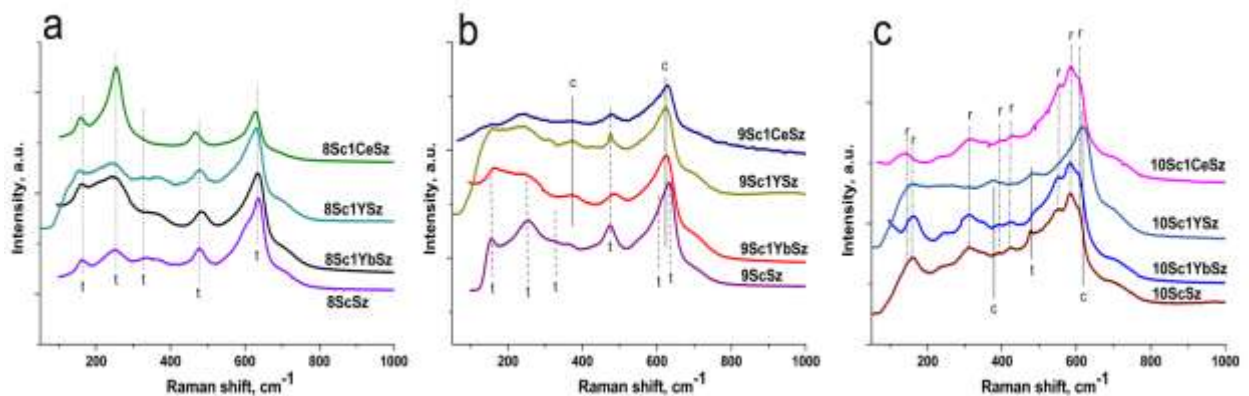


Fig. 2. Raman spectra for crystals 8Sc1RSZ (a), 9Sc1RSZ (b), 10Sc1RSZ (c), where R = Yb, Y, Ce

For 8ScSZ crystals, co-doped with 1 mol% of Yb_2O_3 , Y_2O_3 or CeO_2 the Raman spectra contain lines characteristic of the tetragonal phase based on ZrO_2 [23]. The Raman spectra of the 9Sc1YSZ and 9Sc1CeSZ crystals are similar to the spectrum characteristic of the tetragonal structure, but the lines are substantially broadened, which may be due to the presence in these crystals of

the second phase – cubic – except the tetragonal phase. The Raman spectra of 10ScSZ, 10Sc1YbSZ and 10Sc1CeSZ crystals contain lines corresponding to the rhombohedral phase [23], which are substantially broadened, which may be due to the presence in these crystals of the second phase – cubic.

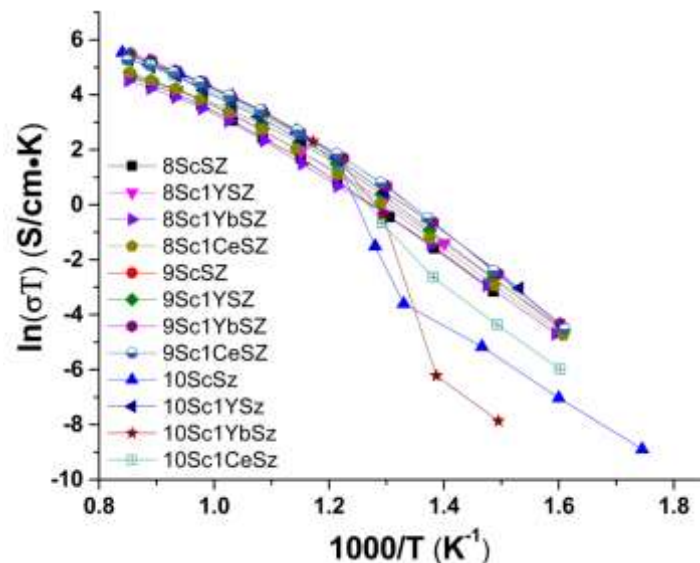


Fig.3. Temperature dependences of the specific conductivity of crystals

The spectra of cubic crystals 9Sc1YbSZ, 10Sc1YSZ are similar to each other and contain peaks corresponding to cubic phase [23-24]. The spectra of these crystals also contain a peak located at $\sim 480 \text{ cm}^{-1}$, which the authors of a number of studies [24-26] attributed to the t'' -phase. The t'' -phase is characterized by the axial ratio $c/a = 1$ and a small displacement of oxygen ions along the c-

axis, which leads to a tetragonal symmetry (space group of $P4_2/nmc$). The t'' -phase is observed in arc-melted $\text{ZrO}_2\text{-Y}_2\text{O}_3$ samples [24], thermal barrier coatings [27] and films of solid electrolytes [28].

Figure 3 in the Arrhenius coordinates shows the temperature dependences of the specific conductivity of the crystals under study.

On the graph of the temperature dependence of the specific electrical conductivity of 10ScSZ, 10Sc1YbSZ and 10Sc1CeSZ crystals in the temperature range of 450-600°C, a break is observed due to the phase transition of the rhombohedral phase to the cubic one. The break in the temperature dependence of the conductivity of 10ScSZ crystals occurs at higher temperatures than in samples 10Sc1YbSZ and 10Sc1CeSZ. This indicates that the introduction of 1 mol% of Yb₂O₃ or CeO₂ in 10ScSZ crystals shifts the range of existence of the rhombohedral phase towards lower temperatures.

Figure 4 shows the dependence of the specific electrical conductivity of crystals at a

temperature of 900°C, depending on the content of Sc₂O₃.

As follows from figure 4, the increase in the content of Sc₂O₃ in the composition of crystals, co-doped with Y₂O₃, Yb₂O₃, and CeO₂, basically leads to an increase in the conductivity of the crystals. For crystals co-doped with 1 mol% of Yb₂O₃, the concentration dependence has a maximum when the content of scandium oxide is 9 mol%. In the case of co-doping with 1 mol% of Y₂O₃, a noticeable increase in conductivity is observed only at a content of 10 mol% Sc₂O₃. In crystals co-doped by 1 mol% of CeO₂, the conductivity of crystals monotonously increases with increasing Sc₂O₃ content.

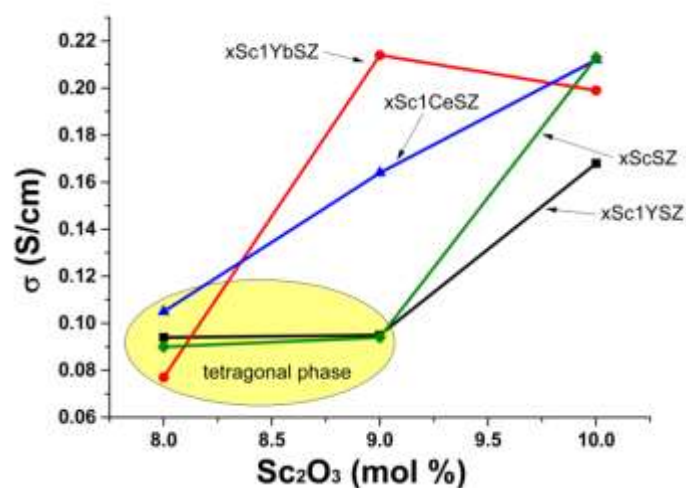


Fig. 4. Comparison of the ionic conductivity of crystals ScSZ, 8Sc1RSZ, 9Sc1RSZ, 10Sc1RSZ, where R-Yb, Y, Ce at a temperature of 900°C

The introduction of 1 mol% of co-doping oxide into 8ScSZ changes the conductivity of crystals in a narrow range of values from 0.08 to 0.10 S/cm, which is associated with the phase composition of the crystals, which practically does not change with the introduction of 1 mol% of the co-doping impurity and consists mainly from the tetragonal phase. Crystals of 9ScSZ, 9Sc1YSZ, in which the tetragonal phase also dominates, have similar conductivity values. Thus, the conductivities of co-doped tetragonal crystals at a temperature of 900°C are close and equal to about 0.1 S/cm.

The introduction of 1 mol% of a co-doping oxide into the 9ScSZ crystals leads to

an increase in the crystal's conductivity but depends on the type of the co-doping oxide. So the conductivity of 9Sc1YSZ crystals is almost comparable to the conductivity of 9ScSZ. The introduction of 1 mol% of CeO₂ in the composition of 9ScSZ crystals leads to an increase in conductivity and the conductivity of 9Sc1CeSZ crystals is approximately 1.5 times higher than the conductivity of 9ScSZ crystals at a temperature of 900°C. The introduction of 1 mol% Yb₂O₃ in the composition of 9ScSZ crystals leads to the most significant changes in the crystal's conductivity. Single-phase pseudo-cubic crystals 9Sc1YbSZ have the maximum conductivity value (0.214 S/cm) among the

doped crystals in the studied range of compositions.

The introduction of 1 mol% co-doping oxide into the composition of 10ScSZ solid solutions leads to a decrease in the conductivity of the crystals. The conductivity values of two-phase crystals containing a mixture of cubic and rhombohedral phases (10ScSZ, 10Sc1CeSZ, and 10Sc1YbSZ) at a temperature of 900°C are close and equal to ~0.2 S/cm. The introduction of 1 mol% Y₂O₃ in the composition of 10ScSZ crystals leads to a noticeable decrease in the crystal's conductivity, despite the fact that the 10Sc1YSZ crystals are single-phase pseudocubic (t''-phase).

The conductivity of 10Sc1YSZ crystals is less than the conductivity of 9Sc1YbSZ crystals with a similar crystal structure. Such a difference in the conductivity values can be associated with a large Y³⁺ ionic radius compared to Yb³⁺ ($R_{Y^{3+}} = 1.019$ and $R_{Yb^{3+}} =$

0.985) and a larger difference with the sizes of the ionic radii of zirconium and scandium ($R_{Zr^{4+}} = 0.84$; $R_{Sc^{3+}} = 0.87$). The introduction of a larger ion in the heterovalent substitution leads to an increase in the lattice stresses, which reduce the conductivity. In addition, crystals 10Sc1YSZ and 9Sc1YbSZ differ in the total concentration of stabilizing oxides (11 and 10 mol%, respectively). An increase in the total concentration of stabilizing oxides above a certain threshold value, which depends on the type of stabilizing impurity, leads to a decrease in conductivity due to the formation of oxygen-ion clusters [29].

It should be noted that the magnitude of the conductivity of 9Sc1YbSZ crystals at a temperature of 900°C is comparable to the same value of 10ScSZ crystals. However, unlike the 10ScSZ crystal containing the rhombohedral phase, the 9Sc1YbSZ sample is a single-phase pseudo-cubic.

Conclusions

Crystals of solid solutions (ZrO₂)_{1-x}(Sc₂O₃)_x (x = 0.08-0.10) doped with 1 mol% Y₂O₃, Yb₂O₃ and CeO₂ were grown by the method of directional crystallization in a cold container. It was shown that homogeneous transparent single crystals were obtained only for the compositions 9Sc1YbSZ and 10Sc1YSZ. It has been detected that stabilization of the cubic phase in crystals co-doped with Yb₂O₃ occurs at a lower concentration of Sc₂O₃ in the solid solution than in crystals soldered with Y₂O₃. Co-doping with cerium oxide did not give the opportunity to obtain a single-phase cubic solid solution.

It is shown that the conductivity of crystals depends on the content of Sc₂O₃ in solid solutions. So, the introduction of 1 mol% of a co-doping oxide into the composition of (ZrO₂)_{0.91}(Sc₂O₃)_{0.09} crystals mainly results in an increase in conductivity. And the introduction of 1 mol% of a co-doping oxide into the composition of (ZrO₂)_{0.9}(Sc₂O₃)_{0.1} crystals reduces the crystal's conductivity.

It is shown that the conductivity values of tetragonal crystals at a temperature of 900°C are close and equal to about 0.1 S/cm.

From the investigated range of compositions, 9Sc1YbSZ crystals have the maximum conductivity in the entire temperature range, conductivity is comparable to the same value for 10ScSZ crystals.

Comparison of various co-doping oxides introduced into (ZrO₂)_{1-x}(Sc₂O₃)_x (x = 0.08 - 0.10) solid solutions to obtain a solid electrolyte with a cubic structure and maximum conductivity in the range of working temperatures of intermediate-temperature SOFC showed that the most promising is the use of as ytterbium oxide dopant. The 10ScSZ crystals have the maximum conductivity, but along with the cubic phase, there is a rhombohedral phase, which leads to the instability of the solid solution at elevated temperatures and degradation of its electrophysical characteristics during long-term operation. 9Sc1YbSZ single-phase crystals possess not only greater phase stability due to the absence of the second phase in them, but doping with ytterbium oxide does not reduce the electrical conductivity, which is comparable to the conductivity of 10ScSZ crystals.

Acknowledgment: This work was financially supported by the Russian Science Foundation grant 16-13-00056 "Development of the Materials Science Fundamentals and Creation of Highly Efficient Oxygen Conducting Membranes for Solid Oxide Fuel Cells". Raman spectroscopy structural technique was developed with the financial support of State Task of Institute of Solid State Physics RAS.

References

1. Badwal S.P.S., Ciacchi F.T., Milosevic D. Scandia-Zirconia Electrolytes for Intermediate Temperature Solid Oxide Fuel Cell Operation. *Solid State Ionics*. 2000, vol. 136–137, pp. 91–99.
2. Kharton V.V., Marques F.M.B., Atkinson A. Transport Properties of Solid Oxide Electrolyte Ceramics: A Brief Review. *Solid State Ionics*. 2004, vol. 174, pp. 35–49.
3. Fergus J.W. Electrolytes for Solid Oxide Fuel Cells. *J. Power Sources*. 2006, vol. 162, pp. 30–40.
4. Yokokawa H., Sakai N., Horita T., Yamaji K., Brito M.E. Solid Oxide Electrolytes for High Temperature Fuel Cells. *Electrochemistry*. 2005, vol. 73, pp. 20–30.
5. Borik M.A., Vishnyakova M.A., Voitsitskii V.P., Kulebyakin A.V., Lomonova E.E., Myzina V.A., Osiko V.V., Panov V.A. Preparation and Properties of Y_2O_3 Partially Stabilized ZrO_2 Crystals. *Inorg. Mater.* 2007, vol. 43, pp. 1223–1229.
6. Osiko V.V., Borik M.A., Lomonova E.E. Synthesis of refractory materials by skull melting, in: Springer hand book of crystal growth. Springer, New York. 2010, pp. 433–477.
7. Borik M.A., Lomonova E.E., Osiko V.V., Panov V.A., Porodinkov O.E., Vishnyakova M.A., Voron'ko Yu.K., Voronov V.V. Partially Stabilized Zirconia Single Crystals: Growth from the Melt and Investigation of the Properties. *J. Cryst. Growth*. 2005, vol. 275, pp. 2173–2179.
8. Berendts S., Lerch M. Growth of yttria-doped zirconium oxide nitride single crystals by means of reactive skull melting. *J. Cryst. Growth*. 2011, vol. 336, pp. 106–111.
9. Badwal S.P.S., Ciacchi F.T., Rajendran S., Drennan J. *Solid State Ionics*. 1998, vol. 109, pp. 167–186.
10. Politova T.I., Irvine J.T.S. Investigation of Scandia–Yttria–Zirconia System as an Electrolyte Material for Intermediate Temperature Fuel Cells—Influence of Yttria Content in System $(Y_2O_3)_x(Sc_2O_3)_{(1-x)}(ZrO_2)_{89}$. *Solid State Ionics*. 2004, vol. 168, pp. 153–165.
11. Du K., Kim C.-H., Heuer A.H., Goettler R., Liu Z. Structural Evolution and Electrical Properties of Sc_2O_3 -Stabilized ZrO_2 Aged at 850°C in Air and Wet-Forming Gas Ambients. *J. Am. Ceram. Soc.* 2008, vol. 91, pp. 1626–1633.
12. Lee D.S., Kim W.S., Choi S.H., Kim J., Lee H.-W., Lee J.H. Characterization of ZrO_2 Co-Doped with Sc_2O_3 and CeO_2 Electrolyte for the Application of Intermediate Temperature SOFCs. *Solid State Ionics*. 2005, vol. 176, pp. 33–39.
13. Abbas H.A., Argirusis C., Kilo M., Wiemhöfer H.D., Hammad F.F., Hanafi Z.M. Preparation and Conductivity of Ternary Scandia-Stabilised Zirconia. *Solid State Ionics*. 2011, vol. 184, pp. 6–9.
14. Omar S., Najib W.B., Chen W., Bonanos N. Electrical Conductivity of 10 mol% Sc_2O_3 –1 mol% M_2O_3 – ZrO_2 Ceramics. *J. Am. Ceram. Soc.* 2012, vol. 95, pp. 1965–1972.
15. Spirin A., Ivanov V., Nikonov A., Lipilin A., Paranin S., Khrustov V., Spirina A. Scandia-Stabilized Zirconia Doped with Yttria: Synthesis, Properties, and Ageing Behavior. *Solid State Ionics*. 2012, vol. 225, pp. 448–452.
16. Lakshmi V.V., Bauri R. Phase formation and ionic conductivity studies on ytterbia co-doped scandia stabilized zirconia ($0.9ZrO_2$ – $0.09Sc_2O_3$ – $0.01Yb_2O_3$)

- electrolyte for SOFCs. *Solid State Sciences*. 2011, vol. 13, pp. 1520-1525.
17. Agarkov D.A., Burmistrov I.N., Tsybrov F.M., Tartakovskii I.I., Kharton V.V., Bredikhin S.I., Kveder V.V. Analysis of interfacial processes at the SOFC electrodes by *in-situ* Raman spectroscopy. *ECS Trans.* 2015, vol. 68, iss. 1, pp. 2093-2103.
 18. Agarkov D.A., Burmistrov I.N., Tsybrov F.M., Tartakovskii I.I., Kharton V.V., Bredikhin S.I. Kinetics of NiO reduction and morphological changes in composite anodes of solid oxide fuel cells: estimate using Raman scattering technique. *Russ. J. Electrochem.* 2016, vol. 52, no. 7, pp. 600-605.
 19. Agarkov D.A., Burmistrov I.N., Tsybrov F.M., Tartakovskii I.I., Kharton V.V., Bredikhin S.I. *In-situ* Raman spectroscopy analysis of the interfaces between Ni-based SOFC anodes and stabilized zirconia electrolyte. *Solid State Ionics*. 2017, vol. 302, pp. 133-137.
 20. Fleig J., Maier J. The impedance of ceramics with highly resistive grain boundaries: validity and limits of the brick layer model. *J. Eur. Ceram. Soc.* 1999, vol. 19, pp. 693-696.
 21. Кузьминов Ю.С., Ломонова Е.Е., Осико В.В. Тугоплавкие материалы из холодного тигля. Москва, Наука. 2004. 374 с.
 22. Andrievskaya E.R. Phase equilibria in systems of oxides of hafnium, zirconium, yttrium with oxides of rare-earth elements. Kiev: Naukova Dumka. 2010, 471 с.
 23. Fujimori H., Yashima M., Kakihana M., Yoshimura M. Structural Changes of scandia-Doped Zirconia Solid Solutions: Rietveld Analysis and Raman Scattering. *J. Am. Ceram. Soc.* 1998, vol. 81, pp. 2885-2893.
 24. Yashima M., Ohtake K., Kakihana M., Arashi H., Yoshimura M. Determination of Tetragonal-Cubic Phase Boundary of $Zr_{1-x}R_xO_{2-x/2}$ (R = Nd, Sm, Y, Er and Yb) by Raman Scattering. *J. Phys. Chem. Solids*. 1996, vol. 57, pp. 17-24.
 25. Hemberger Y., Wichtner N., Berthold C., Nickel K.G. Quantification of Ytria in Stabilized Zirconia by Raman Spectroscopy. *Int. J. Appl. Ceram. Technol.* 2016, vol. 13, pp. 116-124.
 26. Yashima M., Kakihana M., Yoshimura M. Metastable-Stable Phase Diagrams in the Zirconia-Containing Systems Utilized in Solid-Oxide Fuel Cell Application. *Solid State Ionics*. 1996, vol. 86, pp. 1131-1149.
 27. Krogstad J.A., Krämer S., Lipkin D.M., Johnson C.A., Mitchell D.R., Cairney J.M., Levi C.G. Phase Stability of t'-Zirconia-Based Thermal Barrier Coatings: Mechanistic Insights. *J. Am. Ceram. Soc.* 2011, vol. 94, pp. 168-177.
 28. Butz B., Kruse P., Störme H., Gerthsen D., Müller A., Weber A., Ivers-Tiffée E. Correlation between microstructure and degradation in conductivity for cubic Y_2O_3 -doped ZrO_2 . *Solid State Ionics*. 2006, vol. 177, pp. 3275-3284.
 29. Arachi Y., Sakai H., Yamamoto O., Takeda Y., Imanishai N. Electrical conductivity of the $ZrO_2-Ln_2O_3$ (Ln-lanthanides) system. *Solid State Ionics*. 1999, vol. 121, pp. 133.

ТРАНСПОРТНЫЕ ХАРАКТЕРИСТИКИ КРИСТАЛЛОВ ТВЕРДЫХ ЭЛЕКТРОЛИТОВ НА ОСНОВЕ $ZrO_2-Sc_2O_3$ СО-ЛЕГИРОВАННЫХ ОКСИДАМИ СКАНДИЯ, ИТТРИЯ, ИТТЕРБИЯ И ЦЕРИЯ

Д.А. Агарков^{1,2,3}, М.А. Борик³, С.И. Бредихин^{1,2,3}, И.Н. Бурмистров^{1,2,3}, А.С. Числов^{3,4},
Г.М. Елисеева¹, В.А. Колотыгин¹, А.В. Кулебякин³, И.Е. Курицына^{1,3}, Е.Е. Ломонова³,
Ф.О. Милович⁴, В.А. Мызина³, Н.Ю. Табачкова^{3,4}

¹Федеральное государственное бюджетное учреждение науки
Институт физики твердого тела Российской академии наук (ИФТТ РАН),
ул. Академика Осипьяна, д. 2, Черноголовка, Московская обл., 142432 Россия

²Федеральное государственное автономное образовательное учреждение высшего образования «Московский физико-технический институт (национальный исследовательский университет)»
Институтский пер., 9, Долгопрудный, Московская обл., 141701 Россия

³Федеральное государственное бюджетное учреждение науки, Институт общей физики имени А.М. Прохорова Российской академии наук (ИОФ РАН),
ул.Вавилова, 38, г. Москва, 119991Россияе-mail: lomonova@lst.gpi.ru

⁴Федеральное государственное автономное образовательное учреждение высшего образования «Национальный исследовательский технологический университет «МИСиС»
Ленинский пр., 4, г. Москва, 119049 Россия

Приведены результаты исследования структуры и ионной проводимости твердых растворов $(ZrO_2)_{1-x}(Sc_2O_3)_x$ ($x = 0.08 - 0.10$), легированных 1 мол.% Y_2O_3 , Yb_2O_3 и CeO_2 . Кристаллы выращивали методом направленной кристаллизации расплава в холодном контейнере. Исследования фазового состава кристаллов проводили методом рентгеновской дифрактометрии и спектроскопии комбинационного рассеяния света. Транспортные характеристики изучали методом импедансной спектроскопии в температурном диапазоне 400–900°C.

Показано, что однородные прозрачные монокристаллы были получены только для составов $(ZrO_2)_{0.89}(Sc_2O_3)_{0.1}(Y_2O_3)_{0.01}$ и $(ZrO_2)_{0.90}(Sc_2O_3)_{0.09}(Yb_2O_3)_{0.01}$. Стабилизация высокосимметричной фазы в кристаллах, солегированных Yb_2O_3 , происходит при меньшей концентрации Sc_2O_3 в твердом растворе, чем в кристаллах, солегированных Y_2O_3 . Со-легирование оксидом церия не позволило получить однофазный кубический твердый раствор.

Показано, что проводимость кристаллов зависит от содержания Sc_2O_3 в твердых растворах. Установлено, что значения проводимости тетрагональных кристаллов при температуре 900°C близки и составляет величину порядка 0.1 См/см. Из исследуемого диапазона составов максимальную проводимость во всем температурном интервале имеют кристаллы $(ZrO_2)_{0.9}(Sc_2O_3)_{0.09}(Yb_2O_3)_{0.01}$. Величина проводимости данных кристаллов при температуре 900°C сопоставима с аналогичным значением для кристаллов $(ZrO_2)_{0.9}(Sc_2O_3)_{0.1}$. Однако, в отличие от кристалла $(ZrO_2)_{0.9}(Sc_2O_3)_{0.1}$, содержащего ромбоэдрическую фазу, образец $(ZrO_2)_{0.90}(Sc_2O_3)_{0.09}(Yb_2O_3)_{0.01}$ является однофазным псевдокубическим.

Ключевые слова: диоксид циркония, ZrO_2 - Sc_2O_3 , рост кристаллов, ионная проводимость, твердые электролиты, легирование, фазовый анализ

SKANDIUM, İTTRIUM, İTTERBIUM VƏ SERIUM İLƏ LEGİRƏ OLUNMUŞ ZrO_2 - Sc_2O_3 ƏSASINDA BƏRK ELEKTROLİTLƏRİN KRİSTALLARININ NƏQLİYYAT XARAKTERİSTİKALARI

D.A. Aqarkov^{1,2,3}, M.A. Borik³, S.I. Bredixin^{1,2,3}, I.N. Burmistrov^{1,2,3}, A.S. Çislov^{3,4},
Q.M. Eliseeva¹, V.A. Kolotqin¹, A.V. Kulebyakin³, I.E. Kuritsina^{1,3}, E.E. Lomonov³,
F.O. Miloviç⁴, V.A. Mızina³, N.Yu. Tabaçkova^{3,4}

¹Rusiya EA Bərk cisimlərin fizikası institutu

²Moskva fizika-texniki institutu

³Rusiya EA Ümumi fizika institutu

⁴Rusiya milli tədqiqat texnoloji universiteti

Y_2O_3 , Yb_2O_3 u CeO_2 ilə legirə olunmuş $(ZrO_2)_{1-x}(Sc_2O_3)_x$ ($x = 0.08 - 0.10$) bərk məhlulların strukturu və ion keçiriciliyi tədqiq edilib. Müəyyən edilib ki, şəffaf monokristallar yalnız $(ZrO_2)_{0.89}(Sc_2O_3)_{0.1}(Y_2O_3)_{0.01}$ və $(ZrO_2)_{0.90}(Sc_2O_3)_{0.09}(Yb_2O_3)_{0.01}$ tərkiblər üçün alınır. Kristalların keçiriciliyi bərk məhlullarda Sc_2O_3 miqdarından asılıdır. Tədqiq olunan tərkib diapazonunda bütün temperatur intervalında maksimal keçiricilik $(ZrO_2)_{0.9}(Sc_2O_3)_{0.09}(Yb_2O_3)_{0.01}$ kristallarında müşahidə olunur.

Açar sözlər: sirkonium dioksid, ZrO_2 - Sc_2O_3 , ion keçiriciliyi, bərk elektrolitlər, legirləmə, faza analizi.